Surface phonons of the Si(111):In-(4×1) and (8×2) phases

K. Fleischer,[1,2] S. Chandola,[1,2] N. Esser,[3] W. Richter,[2,4] and J. F. McGilp[1]
[1]*School of Physics, Trinity College Dublin, Dublin 2, Ireland*
[2]*Institut für Festkörperphysik, Technische Universität Berlin, Hardenbergstrasse 36, D-10623 Berlin, Germany*
[3] *Department Berlin, Institute for Analytical Sciences (ISAS), Albert-Einstein Strasse 9, 12489 Berlin, Germany*
[4]*INFM, Universitá di Roma Tor Vergata, Via della Ricerca Scientifica 1, I-00133 Roma, Italy*
(Received 12 March 2007; revised manuscript received 16 August 2007; published 7 November 2007)

The reversible phase transition of the Si(111):In-(4×1) surface has been studied using Raman spectroscopy and the symmetry, frequencies, and linewidths of the surface phonon modes have been determined. Dramatically different behavior has been identified for vibrational motion in the direction of the In chains and orthogonal to them. The differences in the Raman spectra of the room and low temperature surface are discussed in terms of the Peierls transition model and a recent dynamical soft shear distortion model. The measurements are found to be consistent with the former model, while some difficulties arise for the latter model. A combined Peierls transition and soft shear distortion model is consistent with the data, but is lacking detail. The Raman spectra presented here represent a challenge in developing theoretical models of this complex system.

DOI: 10.1103/PhysRevB.76.205406 PACS number(s): 73.20.Mf, 73.63.Nm, 78.30.−j, 78.67.Lt

I. INTRODUCTION

In recent years, the physical realization of quasi-one-dimensional (quasi-1D) systems on surfaces has stimulated investigations on the nature of 1D metallic states, as unusual properties such as spin charge separation or charge density waves are expected.[1–3] One interesting system is the Si(111):In-(4×1) surface, which is known to be a 1D conductor at room temperature but changes to a nonconducting phase at low temperatures.[4,5] In the accepted model of the Si(111):In-(4×1) surface, two zigzag rows of In atoms form quasi-1D chains, separated by a zigzag row of Si atoms (see Fig. 1).[6] The reversible phase transition of this quasi-1D system into an (8×2) geometry at temperatures below 120 K has attracted considerable interest in recent years.[4,6–18] The nature of the transition is still not fully understood and several models are currently under discussion: a single or triple band Peierls transition,[4,10,13,14,17] an order-disorder phase transition where the room temperature (RT) (4×1) phase is explained by a thermal mixture of different (4×2) sub-unit-cells,[11] a displacive phase transition involving entirely different structures,[8] and, most recently, an order-disorder phase transition involving a soft shear distortion between asymmetric ground states, where the RT (4×1) symmetry is explained as a time average of the whole surface.[15] Although initially the theoretical low temperature (LT) model did not identify the semiconducting nature of the (8×2) phase—in contrast to the models for the 1D metallic (4×1) phase—recently published new models appear to describe the band structure of the (8×2) phase quite well.[13–15] However, there is still considerable dispute about the physical description of the room temperature phase either as a fluctuating average of LT unit cells or as a thermodynamic stable phase[15,16,19,20]

The prediction of soft phonon modes by González *et al.*[15] and the availability of density functional theory calculations of the surface phonon modes of the (4×1) phase[21] have stimulated the more detailed Raman spectroscopy studies of the surface phonon modes of both phases reported in this paper, where particular attention is paid to the symmetry of the modes and the low energy In-In vibrations crucial for the understanding of the surface phase transition. The changes in the Raman spectra upon cooling are described and, after the usual temperature related shift of phonon modes is identified, the changes arising from the phase transition are discussed in terms of the different models. The observed surface phonon modes for both phases are listed, together with their symmetry.

II. EXPERIMENT

The measurements were performed in a UHV system of base pressure 8×10^{-11} mbar, equipped with a liquid helium cooling stage with integrated direct current heating and a standard Knudsen cell for In evaporation. The vicinal Si(111) samples, with an offcut of 1° toward the $[\bar{1}\,\bar{1}2]$, were heat treated at 1100 °C following the method described by Viernow *et al.*[22]

The formation of the single domain (4×1) surface was monitored *in situ* with reflection anisotropy spectroscopy and confirmed with low energy electron diffraction, as described elsewhere.[12,23] Modifications to the chamber (preparation di-

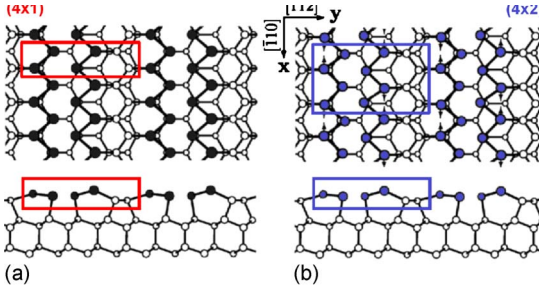

FIG. 1. (Color online) Schematic of the (a) (4×1) and (b) (4×2) structures from the model of Wang *et al.* (Ref. 7). The unit cells are marked as well as the 6 (12) atoms in the first double layer that dominate the low frequency microscopic surface modes.

rectly on the cooling stage) avoided the problem of the suppression of the phase transition by contamination[12,24] and also allowed the sample reorientation necessary to determine the symmetry of the surface phonon modes using Raman selection rules. The chain direction ($[\bar{1}10]$) is defined as x, the perpendicular direction $[\bar{1}\,\bar{1}2]$ as y, and the surface normal as z (see also Fig. 1). Following the Porto notation $[\boldsymbol{k}_i(\boldsymbol{e}_i,\boldsymbol{e}_s)\boldsymbol{k}_s]$, measurements were performed in $z(y,y)\bar{z}$ and $z(x,y)\bar{z}$, probing the A' and A'' symmetries respectively.[25] These two fundamental symmetries arise from the $1m$ (C_s) symmetry of the (4×1) and (8×2) surfaces, showing only one mirror plane, perpendicular to the In chains (yz plane in our notation). In such a system, only two classes of symmetry allowed vibrational modes exist, those within the mirror plane (A') and those perpendicular to it (A'').

The Raman spectrometer consists of a DILOR-XY triple-grating monochromator with a slit width of 150 μm operating in subtractive mode for efficient reduction of the elastically scattered background, together with a LN_2 cooled charge coupled device (CCD) Array (Spectrum-1, F36, CCD 1024×256-0). Spectra shown in the first sections were taken with a Kr^+ ion laser operated at 647 nm (1.91 eV) and 90 mW, using a 250 μm spot size. The resolution in this configuration is about 1.5 cm^{-1}. For the resonance measurements, lines from both the Kr^+ laser and an Ar^+ laser were used. In order to minimize the elastically scattered background, it was necessary to select sample areas with few macroscopic defects: a camera at the entrance slit of the monochromator allowed this to be monitored. Modes with phonon energies as low as 20 cm^{-1} were identified under these conditions. In contrast to earlier measurements on the surface phonons with high resolution electron-energy-loss spectroscopy (HREELS),[9] this enables the low energy In-In and In-Si vibrations to be probed directly.

III. RESULTS

A. Two phases and the phase transition

The Raman spectra of the (4×1) and (8×2) phases for different polarization geometries are shown in Fig. 2, while Fig. 3 shows the development of the spectra taken during cooling at 1 K/min. A large number of surface modes are found for this particular surface (see full list in Sec. III B). It is generally agreed that the (4×1) phase has a unit cell comprising four In and two Si in the first and eight Si atoms in the second double layer (see Fig. 1). Making the simplifying assumption that the underlying Si atoms show bulklike behavior,[21] the six atoms in the first double layer give 12 modes of A' and 6 of A'' symmetry. The Raman effect probes phonons around the Γ point of the Brillouin Zone, and two of these modes (within an essentially two dimensional translational symmetry) are expected to be acousticlike and not observable. It should be noted, however, that bulklike layers have been shown previously to contribute significantly to the surface vibrational modes [see, for instance, Sb on InP (Refs. 25 and 26)]. The degree of confinement to the surface may vary for the different eigenmodes and thus the description of surface eigenmodes in terms of the top layer of atoms of Fig. 1 may be a significant approximation.

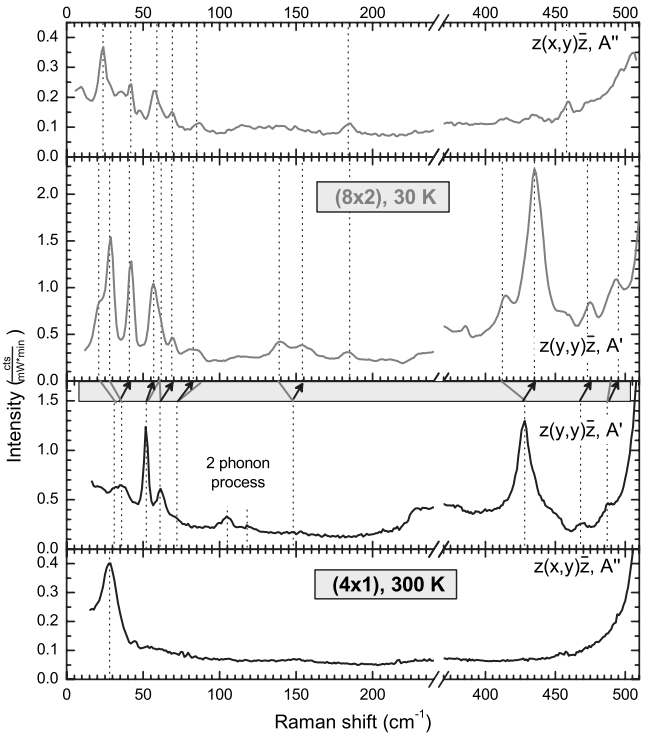

FIG. 2. Raman spectra of the (4×1) and (8×2) phases taken in A' and A'' symmetries, using an incident laser energy of 1.91 eV. The positions of the Raman modes are marked by dotted lines (see also Table I). New (8×2) modes, assigned to backfolding of the phonon branches, are indicated by gray lines, while blueshifting of modes on cooling is marked by black arrows. The spectral range from 240 to 370 cm^{-1} is omitted as it is dominated by the bulk Si 2TA structure.

Nine modes are easily identified in measurements probing A' symmetry, together with two weaker modes assigned to a two phonon process (see Fig. 2). Some of these modes are asymmetrically broadened, indicating modes that are not resolved. In contrast to the rich A' structure, only one broad mode with A'' symmetry is seen for the RT phase.

The phase transition was monitored by slowly cooling the samples at 1 K/min and recording the spectra with a short integration time of 4 min. In Fig. 3, the spectra for 250 and 60 K are shown directly for comparison, while all the others are shown as a gray scale, using white for the highest intensity. Cooling is expected to produce a small blueshift of the phonon modes, accompanied by an increase in intensity. This is most clearly seen for the mode at 428 cm^{-1}, which shifts to 435 cm^{-1}. The intensity of this mode initially increases with cooling but, below the phase transition at 120 K (Fig. 3), it decreases again. This reduction in spectral weight is consistent with a splitting of the mode arising from the backfolding that accompanies the doubling of the real space unit cell. For weakly dispersing modes, formation of the LT phase will produce new modes in the vicinity of the original modes. Strongly dispersing modes will produce new modes at positions far from those of the RT phase (e.g., 266 cm^{-1}).

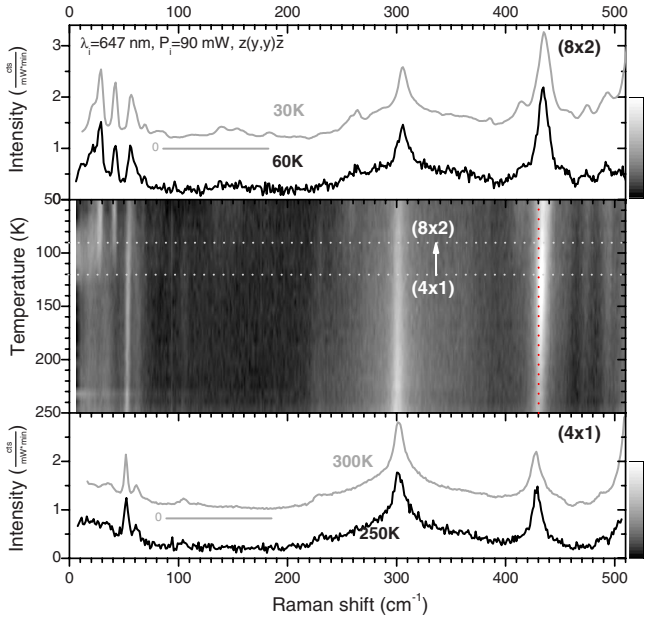

FIG. 3. (Color online) Raman spectra of the (4×1) (bottom) and (8×2) phases (top). The integration time for the high quality measurements was 20 min. The spectra taken during cooling at −1 K/min used a 4 min integration time to enable the phase transition to be monitored (examples are shown at 250 and 60 K, with the overall intensity expressed as a gray scale).

The (8×2) unit cell should produce many more observable modes, if there is significant electronic interchain interaction. However, if the dominant Raman modes are localized within the chains, measurable differences in the phonon energies above 20 cm^{-1} between the (8×2) and the smaller (4×2) unit cell would not be expected. As no phonon calculations of mode energies and their displacement vectors exist for the low temperature (8×2) structure, detailed discussion will be limited to the simpler (4×2) unit cell.

The 4×2 sub-unit-cell [Fig. 1(b)] has 24 A' and 12 A'' modes, including two nonobservable, acousticlike modes. Figure 2 shows that many of these modes are resolved (17 A' and 8 A'' modes). Some smaller structures seen in the spectra for 1.91 eV incident energy could not be confirmed with other laser lines, due to poorer resolution, and are omitted from the list in Tables I and II.

B. Surface modes

As the intensity of the surface phonons is weak, care is required in assigning measured structures. Due to the large integration time needed, systematic errors, such as weak plasma lines or artificial lines created by excitations due to cosmic background radiation, may produce artifacts. Such problems can be minimized by comparing measurements taken at different incident laser energies (see Fig. 4). An individual measured peak was only assigned to a surface phonon mode if it was identified for all measured laser energies, as this procedure eliminates plasma lines.

Table I lists the identified modes of the (4×1) surface. For the (8×2) surface, the increased number of modes is a further complication. Table II lists the identified modes using the same procedure as for the (4×1) surface. In both tables, modes are indicated where the measurements at lower incident laser energy (1.91 and 1.83 eV), and thus better resolution, suggest that more than one mode contributes to the measured peak.

TABLE I. List of the identified surface phonon modes of the Si(111)-In:(4×1) surface. The fitting procedure is described in the text. The FWHM of the modes, $2w_L$, is the Lorentzian width. Some modes have unusually large FWHMs and large errors in the frequency determination. More than one mode may be contributing, but no definite assignment is possible as these modes are either weak (148 cm^{-1}) or only shoulders on stronger modes (36, 72 cm^{-1}).

Symmetry	ω_0 (cm^{-1})	$2w_L$ (cm^{-1})	Comments
A''	28±0.9	10±2	
A'	31±1	6±4	1.91 and 1.83 eV only
	36±2	14±10	Possibly two modes
	51.8±0.6	3±1	
	61±1.3	5±2	
	72±3.3	11±9	Possibly two modes
	105±1	8±3	Two phonon
	118±1	9±2	process
	148±7	16±12	Possibly two modes
	428±1	14±4	Resonant to 2TA(W)
	467±1.5	7±7	1.91 and 1.83 eV only
	487±2.6	10±2	1.91 and 1.83 eV only
Γ'_{25}	520.0±0.2	2.5±0.2	Si bulk

The data of Fig. 4 were fitted using a multipeak analysis of Voigt profiles resulting from a convolution of Gaussian and Lorentzian curves. The Gaussian broadening, attributed to the instrumental resolution, was determined by measuring a plasma line of the ion laser for each incident laser energy and was kept constant for all modes ($2w_G$: 1.9, 2.2, 3.6, 3.8, 4.8 cm^{-1} for incident laser energies of 1.83, 1.91, 2.18, 2.41, 2.54 eV, respectively). In Tables I and II, only the Lorentzian width of the phonon lines is given. The elastically scattered background from the incident laser beam was approximated by an exponential decay. The errors in the energy were estimated from the confidence interval of the fits, together with the standard deviation of the position derived from the individual fits at different laser energies. The latter is necessary as variations in focusing conditions and coupling into the monochromator, which cannot be avoided when using a macro-Raman system attached to a UHV chamber, can lead to shifts in the energy axis (the errors are larger than those of a dedicated micro-Raman spectrometer).

IV. DISCUSSION

A. Assignment of modes

Allowing for the blueshift on cooling, comparison of Tables I and II shows that most modes of the (4×1) struc-

TABLE II. List of the identified surface phonon modes of the Si(111)-In:(8×2) surface. The spectra with the highest resolution and signal-to-noise ratio (1.91 eV) indicate that more than one structure may be contributing for several of the modes. The larger errors, compared to the RT measurements, in energy and Lorentzian linewidth $2w_L$, are a consequence of the large number of peaks fitted.

Symmetry	ω_0 (cm^{-1})	$2w_L$ (cm^{-1})	Comments
A''	23.5±0.8	4±1.5	Possibly two modes
	42±3.5	8±5	Possibly three modes
	59±3	8±6	Possibly two modes
	69±1.5	4±1.5	
	85±1.7	8±4	
	184±0.7	7±3	
	262±2	12±7	
	458±1.2	3±1.5	
A'	21±1.6	4±3	
	28±1.3	4±2	
	41±2	4±2	
	57.2±0.7	5±2	
	62±1.5	3±4	
	69±1.1	5±4	
	83±2.3	7±6	Possibly two modes
	100-130		Broad structure
	139±1.2	11±6	Possibly two modes
	154±2	7±6	Possibly two modes
	185±2	12±8	Possibly two modes
	255±4	7±6	
	264±3	7±4	Also in HREELS[a]
	412±2.5	10±8	
	435.1±0.7	22±10	Resonant to 2TA(W)
	473±2	4±4	Also in HREELS[a]
	495±5	18±14	Also in HREELS[a]
Γ'_{25}	523.6±0.8	0.9±0.2	Si bulk

[a]Reference 9.

ture also appear in the (8×2) spectra. Only two modes occur exclusively on the (4×1) surface (105, 118 cm^{-1}), and these assigned to two phonon structures of the 51.8±0.6 and 61±1.3 cm^{-1} modes. Such a two phonon scattering process is more likely at higher temperature due to the higher occupation number of the phonon modes. At LT, such modes will become weaker, as can be seen in Fig. 3 for the peak in the Si 2TA structure at 300 cm^{-1} [2TA(X)]. Resonance studies, and the determination of the symmetry of the strong (4×1) mode at 428 cm^{-1} [435 cm^{-1} for the (8×2) surface], suggest a new assignment of this mode, which was assigned previously to a microscopic vibration of the Si zigzag chain.[12] Resonance studies reveal that the width and intensity of this mode and the Si bulk 2TA structure are correlated. Even high resolution measurements using the additive mode of the triple-grating monochromator do not significantly change the line shape. The width of this structure remains large, particularly at incident laser energies above 2 eV, compared with the linewidth of the low energy modes or the Si bulk Γ_{25} mode (see Table I). It is therefore likely that a surface resonance is enhancing the 2TA(W) bulk structure located around 430 cm^{-1},[27] and that this is dominating the response.

The rest of the modes are assigned to surface vibrations. Table I lists 8 A' modes but only a single A'' mode for the (4×1) structure, while Table II lists 15 A' modes and 8 A'' modes for the (8×2) structure. Individual phonon modes have been calculated for the (4×1) structure,[21] but direct assignment is difficult because the calculations include the underlying Si layers, leading to a very large number of modes. However, some general conclusions can be drawn. The calculation shows that all low energy modes (<70 cm^{-1}) are dominated by In-In vibrations, while modes above 250 cm^{-1} are dominated by Si-Si vibrations. The In-In modes are of major interest, as the phase transition is accompanied by a change in the In-In interatomic distances.[8] Table I lists five A' In-In vibration modes perpendicular to the chains, but only one broad A'' In-In mode associated with vibrations along the chain direction. No A'' modes are observed above 70 cm^{-1}. For the larger unit cell of the (8×2) surface, more modes are observed, most above 70 cm^{-1} at energetic positions consistent with backfolding of weakly dispersing phonon branches and/or small changes in In-In interatomic distances. The rather weak A' (4×1) mode at 36±2 cm^{-1} splits into two strong modes at 28±1.3 and 41±2 cm^{-1}, giving one additional A' mode below 70 cm^{-1} (Table II). In the chain direction, the changes are much more dramatic, with four A'' modes below 70 cm^{-1} replacing the single RT mode. The Raman spectra provide direct evidence that In-In vibrations with displacement patterns parallel to the chains change substantially between the two phases, while those with displacements perpendicular to the chains are much less affected.

B. Models for the phase transition

In the absence of supporting calculations, the experimental results on the surface vibrational modes can only exclude one of the phase transition models,[11] but reveal some difficulties with a recent dynamical fluctuation model.[15,20]

Peierls transition model.[4,10,13,17,28] Comparison of the (4×1) and (8×2) Raman spectra reveals that all major modes of the (4×1) surface are found in the (8×2) spectra, though blueshifted and with increased intensity due to the lower temperature. In addition, many new modes are found in the (8×2) spectra, most at energetic positions consistent with a backfolding of weakly dispersing phonon branches when the surface unit cell is doubled in a Peierls-distorted phase. Evidence of a dynamical charge density wave (CDW), consistent with a Peierls instability, has been obtained directly from scanning tunneling microscopy measurements of the LT phase.[28]

Individual chains are known to undergo the phase transition over a range of temperatures due to defects within the chain and also because of temperature gradients.[4,28] The Ra-

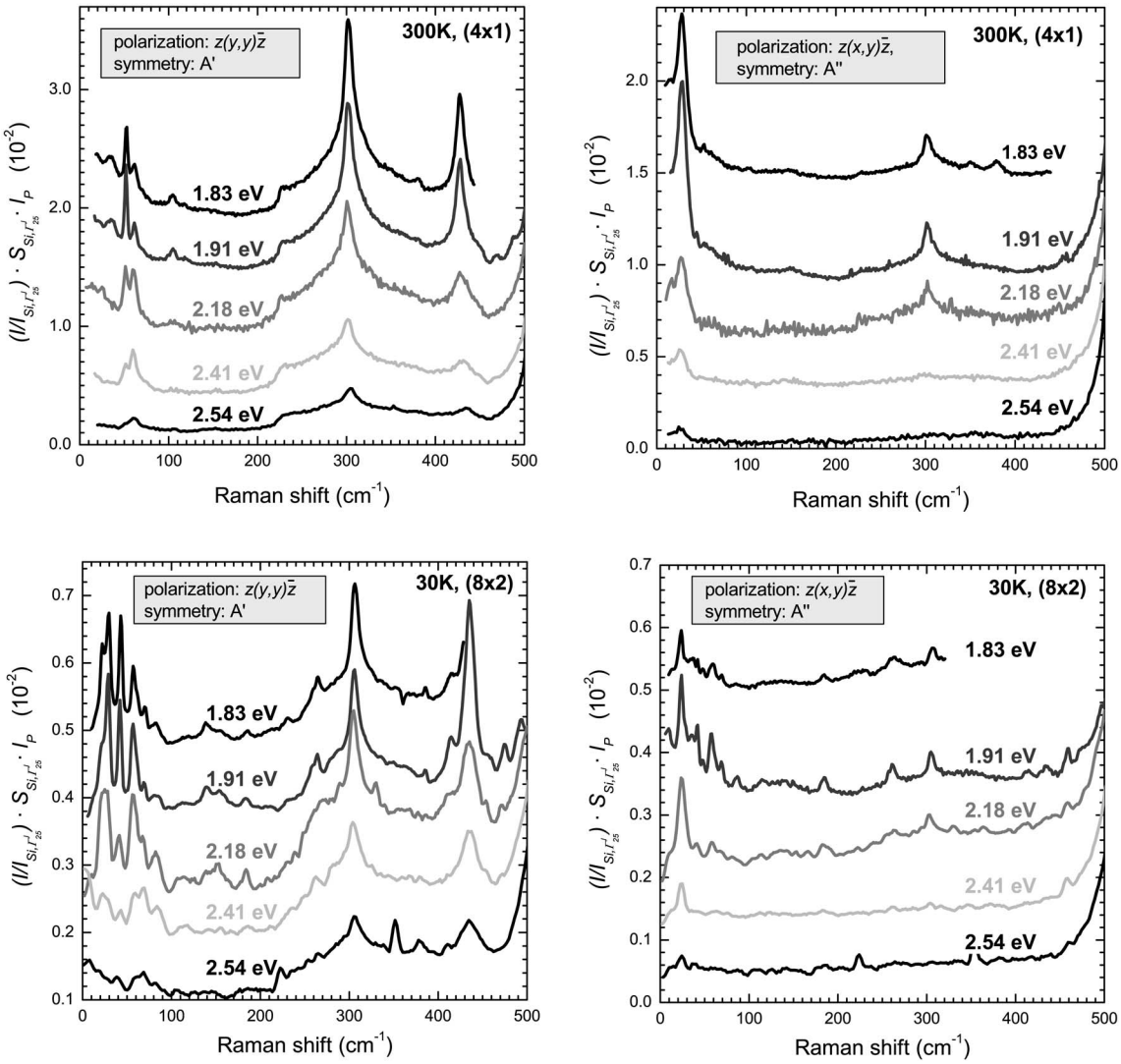

FIG. 4. Spectra of the Si(111):In-(4×1) and (8×2) surfaces taken at different incident laser energies. The spectra are normalized by the intensity of the Si bulk phonon mode, which was corrected for the variation in penetration depth and the bulk resonance response.

man spectra in the temperature range from 120 to 90 K (Fig. 5) appear to be a simple linear combination of the (8×2) and (4×1) spectra, in agreement with this model.

Finally, the observed sensitivity of the surface to very small amounts of additional In (Refs. 24 and 29) is also consistent with this model, as adsorbates prevent the formation of nonlocal collective states such as the CDW. The observation that the formation of the LT (8×2) phase is suppressed by the adsorption of <0.1 ML In is consistent with the Peierls model.[12]

Order-disorder transition models.[11,15] An early order-disorder transition model postulates that the RT structure is an average of spatially disordered, LT (4×2) sub-unit-cells.[11] Raman spectroscopy probes local vibrational modes and thus would detect the presence of such sub-unit-cells. No evidence of the LT vibrational signature is found at RT, allowing this model to be excluded.

A more recent order-disorder model invokes a soft phonon mode, associated with a shear distortion, that moves the In atoms dynamically between asymmetrically distorted (8×2) structures, with a finite occupation time in a symmetric (4×1) structure at RT. At LT, the system is frozen into one asymmetric distorted hexagonal structure.[15,20] At RT, the model predicts that the spectral weight of the contributing asymmetric (8×2) structures is still comparable to the symmetric (4×1) structure.[19,20] Consequences for the Raman spectra would be, first, that the (8×2) structure should have distinctively different vibrational spectra from the symmetric (4×1) structure. Second, the signatures of the LT structures should be found in the RT spectra. Third, as the RT phase is formed, the order-disorder transition should produce broadening of Raman lines, which is well documented in other systems.[30,31] Fourth, soft phonon modes should show characteristic shifts in energy around the transition temperature, although this is not a unique feature of an order-disorder transition, as similar soft modes have been found in Peierls systems.[32–35]

The Raman data show more peaks in the LT spectrum than in the RT spectrum, clearly ruling out a spectral signature of the LT structure at RT (contradicting point 2, but in

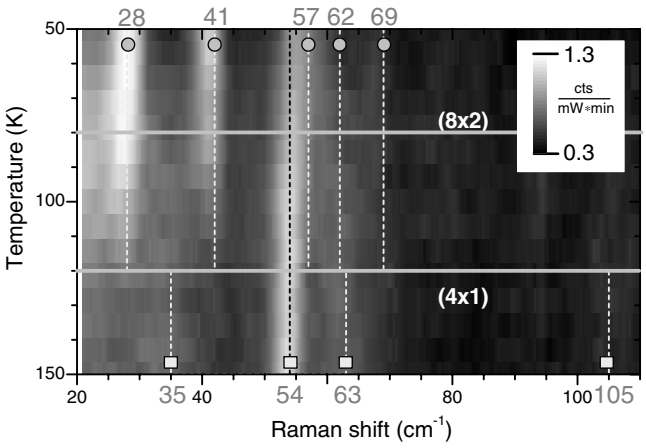

FIG. 5. Low energy region of the A' symmetry spectrum in the temperature range between 150 and 50 K. The gray scale is changed from Fig. 3 to improve the contrast. The dotted lines mark the position of the phonon modes at 150 K for the (4×1) phase and at 50 K for the (8×2) phase. The spectrum in the temperature range from 120 to 80 K appears to be a simple linear combination of the two distinct Raman spectra.

agreement with recent photoemission results[16]). The larger number of peaks at LT is consistent with an asymmetric phase (point 1), but the data show a strong relation between the LT and RT structures, in that all the (4×1) lines appear in (8×2) spectra, although blueshifted and more intense, as discussed above. This might be explained by noting that all but one of these lines are of A' symmetry (vibrations orthogonal to the chain direction), and postulating that the effect of the structural asymmetry will appear mainly in vibrations in the shear distortion direction, i.e., along the chains. This might also help to explain, within this model, the narrow linewidths observed for some of the A' modes at RT, which appear to contradict point 3: e.g., the strongest low energy phonon mode at 51.8 ± 0.6 cm^{-1} is of A' symmetry and is very sharp at RT, with a full width at half maximum (FWHM) of only 3 ± 1 cm^{-1}. In contrast, measurement of the A' 36 cm^{-1} mode using the best resolution from a single laser line gives a width of 12 ± 1 cm^{-1}. At LT, this mode shifts to 41 cm^{-1} and narrows to 4 ± 2 cm^{-1}, consistent with point 3. Changes in Raman linewidths at the phase transition could not be monitored, as the signal-to-noise ratio (SNR) of the variable temperature measurements was too poor for reliable peak analysis. Linewidth measurement is also complicated by unresolved side modes in some of the spectral lines (Table II). The insensitivity of particular A' modes to the phase change, while other A' modes are affected, is unusual, but such behavior is observed occasionally for order-disorder transitions in complex bulk materials.[30]

The very different form of the A' and A'' spectra at RT is consistent with the dynamical fluctuation model. The dynamical shear distortion along the chain direction would be expected to broaden and smear out the A'' modes and, indeed, only one broad A'' mode is detected at RT (Table I). A' modes, with motion in the orthogonal direction, would be less affected, and eight surface modes are observed. At LT, the configurations are frozen, revealing more modes of A'' symmetry (Table II). Freezing of soft phonon modes is expected when the average thermal energy, kT, is reduced below the energy of the modes. The onset of the phase transition at 120 K corresponds to $\sim$80 cm^{-1}, close enough to the energy of a number of LT A'' modes (59, 69, 85 cm^{-1}) to support the idea that the freezing in of vibrational A'' modes may be involved in the mechanism of the phase transition.

Regarding soft phonon modes (point 4), their spectral signature of a strong dispersion of mode energy with temperature has been seen in a wide range of structural phase transitions.[32] The low energy region of the A' symmetry spectrum in the temperature range between 150 and 50 K is shown in Fig. 5. The dotted lines mark the position of the phonon modes at 150 K for the (4×1) phase and at 50 K for the (8×2) phase. The spectrum in the temperature range from 120 to 80 K appears to be a simple linear combination of the two distinct Raman spectra. There is no evidence, above 20 cm^{-1}, of the characteristic energy dispersion of a soft phonon mode. However, as discussed above, the main soft mode is predicted to be a shear mode of the two zigzag In chains in the x direction,[15] and thus to be of A'' symmetry. Measurements of the A'' modes require long integration times at 30 K and it is possible that one of them is the predicted soft mode. The poor SNR in A'' geometry prevented temperature dependent, wide spectrum scans and current calculations provide no estimate of the soft mode energy. These energies can be very low, for example, only 30 cm^{-1} for the soft mode spin-Peierls transition in $CuGeO_3$.[34] The absence of evidence of a soft mode is inconclusive in assessing the model. A more significant problem for this model is that it does not explain why adsorption of additional In or other metals of <0.1 ML stabilizes the (4×1) phase at low temperatures.[12,24,29] If the RT (4×1) phase is predominantly a transient structure connecting the basic (8×2) LT sub-unit-cells, whose spectral intensity is still significant at room temperature, contamination seems more likely to lead to a "frozen" randomization of LT sub-unit-cells, instead of the (4×1)-like vibrational structure actually found.[12]

In summary, the Raman results exclude a significant contribution from the LT (8×2) structure in the RT spectra, in agreement with recent photoemission results.[16] No direct evidence of a soft phonon mode was found, but the apparent softening of modes of A'' symmetry, which are associated with vibrations along the chains, leading to only one mode being observable at RT, is consistent with the presence of soft shearing motions in the chain direction.

Combination of Peierls transition and soft shear distortion. In a recent publication by Riikonen *et al.*, the possibility was raised that both mechanisms contribute to the phase transition.[18] The calculated LT structure is in good agreement with measured LT atomic positions[8] and also the semiconducting nature of the phase. If the CDW leads to a periodic lattice distortion, the total energy of the system will be lowered, following Peierls' argument. The calculated (8×2) ground state with the asymmetrical shear distortion could be essentially identical to a lattice distortion consequent on CDW formation. The soft shear modes associated with vibrations in the chain direction then provide a mechanism for the transition to the RT metallic phase.

V. CONCLUSIONS

In measuring the symmetry, frequencies, and linewidths of the surface phonon modes of both phases of the reversible transition of the Si(111):In-(4×1) surface, it has emerged that the symmetry of the modes is particularly important, with dramatically different behavior identified for vibrational motion in the direction of the chains and orthogonal to them. The data are generally consistent with a Peierls transition as the driving force for the reversible phase transition,[4,10,13,17,28] but a detailed theoretical model is required. Recent theoretical calculations leading to an asymmetrical structure for the (8×2) and a dynamical fluctuation for the (4×1) structure suggest an explanation of some of the details of the Raman measurements.[14,15] Specifically, soft shear distortions in the chain direction predicted by this model may explain the single broad mode of A'' symmetry observed at RT, which contrasts with the minimum of 8 sharp A'' modes observed at LT. However, in agreement with recent photoemission results,[16] the spectra do not show the substantial spectral weight of the (8×2) subunits at RT predicted by the model.[19,20] The results also allow an early order-disorder transition model to be excluded.[11] The Raman spectra presented here represent a challenge to current theoretical models of this system.

ACKNOWLEDGMENTS

This paper has emanated from research conducted with the financial support of Science Foundation Ireland, the Irish Research Council for Science, Engineering and Technology, and SFB 290 of the Deutsche Forschungsgemeinschaft. Wolf Gero Schmidt and Friedhelm Bechstedt are thanked for fruitful discussions and sharing their data.

[1] F. J. Himpsel, K. N. Altmann, R. Bennewitz, J. N. Crain, A. Kirakosian, J. L. Lin, and J. L. McChesney, J. Phys.: Condens. Matter **13**, 11097 (2001), and references therein.
[2] J. Voit, Rep. Prog. Phys. **57**, 977 (1994), and references therein.
[3] P. Segovia, D. Purdie, M. Hengsberger, and Y. Baer, Nature (London) **402**, 504 (1999).
[4] H. W. Yeom, S. Takeda, E. Rotenberg, I. Matsuda, K. Horikoshi, J. Schaefer, C. M. Lee, S. D. Kevan, T. Ohta, T. Nagao, and S. Hasegawa, Phys. Rev. Lett. **82**, 4898 (1999).
[5] T. Kanagawa, R. Hobara, I. Matsuda, T. Tanikawa, A. Natori, and S. Hasegawa, Phys. Rev. Lett. **91**, 036805 (2003).
[6] O. Bunk, G. Falkenberg, J. H. Zeysing, L. Lottermoser, R. L. Johnson, M. Nielsen, F. Berg-Rasmussen, J. Baker, and R. Feidenhans'l, Phys. Rev. B **59**, 12228 (1999).
[7] S. Wang, W. Lu, W. G. Schmidt, and J. Bernholc, Phys. Rev. B **68**, 035329 (2003).
[8] C. Kumpf, O. Bunk, J. H. Zeysing, Y. Su, M. Nielsen, R. L. Johnson, R. Feidenhans'l, and K. Bechgaard, Phys. Rev. Lett. **85**, 4916 (2000).
[9] K. Sakamoto, H. Ashima, H. W. Yeom, and W. Uchida, Phys. Rev. B **62**, 9923 (2000).
[10] H. W. Yeom, K. Horikoshi, H. M. Zhang, K. Ono, and R. I. G. Uhrberg, Phys. Rev. B **65**, 241307(R) (2002).
[11] J.-H. Cho, D.-H. Oh, K. S. Kim, and L. Kleinman, Phys. Rev. B **64**, 235302 (2001).
[12] K. Fleischer, S. Chandola, N. Esser, W. Richter, and J. F. McGilp, Phys. Rev. B **67**, 235318 (2003).
[13] S. F. Tsay, Phys. Rev. B **71**, 035207 (2005).
[14] C. González, J. Ortega, and F. Flores, New J. Phys. **7**, 100 (2005).
[15] C. González, F. Flores, and J. Ortega, Phys. Rev. Lett. **96**, 136101 (2006).
[16] J. R. Ahn, J. H. Byun, J. K. Kim, and H. W. Yeom, Phys. Rev. B **75**, 033313 (2007).
[17] J. R. Ahn, J. H. Byun, H. Koh, E. Rotenberg, S. D. Kevan, and H. W. Yeom, Phys. Rev. Lett. **93**, 106401 (2004).
[18] S. Riikonen, A. Ayuela, and D. Sanchez-Portal, Surf. Sci. **600**, 3821 (2006).
[19] H. W. Yeom, Phys. Rev. Lett. **97**, 189701 (2006).
[20] C. González, F. Flores, and J. Ortega, Phys. Rev. Lett. **97**, 189702 (2006).
[21] F. Bechstedt, A. Krivosheeva, J. Furthmüller, and A. A. Stekolnikov, Phys. Rev. B **68**, 193406 (2003).
[22] J. Viernow, J. L. Lin, D. Y. Petrovykh, F. M. Leibsle, F. K. Men, and F. J. Himpsel, Appl. Phys. Lett. **72**, 948 (1998).
[23] F. Pedreschi, J. D. O'Mahony, P. Weightman, and J. R. Power, Appl. Phys. Lett. **73**, 2152 (1998).
[24] S. V. Ryjkov, T. Nagao, V. G. Lifshits, and S. Hasegawa, Surf. Sci. **488**, 15 (2001).
[25] *Light Scattering in Solids VIII: Raman Scattering from Surface Phonons*, edited by M. Cardona and G. Güntherodt (Springer-Verlag, Berlin, 2000).
[26] N. Esser, K. Hinrichs, J. R. Power, W. Richter, and J. Fritsch, Phys. Rev. B **66**, 075330 (2002).
[27] B. A. Weinstein and G. J. Piermarini, Phys. Rev. B **12**, 1172 (1975), and references therein.
[28] S. J. Park, H. W. Yeom, S. H. Min, D. H. Park, and I.-W. Lyo, Phys. Rev. Lett. **93**, 106402 (2004).
[29] K. Fleischer, S. Chandola, N. Esser, and J. F. McGilp, Phys. Status Solidi B **242**, 2655 (2005).
[30] R. Rao, T. Sakuntala, and S. Deb, J. Mol. Struct. **789**, 195 (2006).
[31] H.-G. Unruh, J. Raman Spectrosc. **17**, 113 (1986).
[32] J. F. Scott, Rev. Mod. Phys. **46**, 83 (1974).
[33] E. Mele, Surf. Sci. **278**, 135 (1992).
[34] H. Kuroe, T. Sekine, M. Hase, Y. Sasago, K. Uchinokura, H. Kojima, I. Tanaka, and Y. Shibuya, Phys. Rev. B **50**, 16468 (1994).
[35] A. Girlando, A. Painelli, S. Bewick, and Z. Soos, Synth. Met. **141**, 129 (2004).